Journal of Industrial and Engineering Chemistry 20 (2014) 290–296

Contents lists available at SciVerse ScienceDirect

Journal of Industrial and Engineering Chemistry

journal homepage: www.elsevier.com/locate/jiec

Opto-electrical and density functional theory analysis of poly (2,7-carbazole-alt-thieno[3,4-c]pyrrole-4,6-dione) and photovoltaic behaviors of bulk heterojunction structure

Kwan Wook Song [a], Min Hee Choi [a], Jang Yong Lee [b], Doo Kyung Moon [a,*]

[a] Department of Materials Chemistry and Engineering, Konkuk University, 1 Hwayang-dong, Gwangjin-gu, Seoul 143-701, Republic of Korea
[b] Energy Materials Research Center, Korea Research Institute of Chemical Technology, P.O. Box 107, Yuseong, Daejeon 305-600, Republic of Korea

ARTICLE INFO

Article history:
Received 8 March 2013
Accepted 30 March 2013
Available online 6 April 2013

Keywords:
Organic photovoltaics(OPVs)
Thieno[3,4-c]pyrrole-4,6-dione(TPD)
Unsubstituted and substituted thiophene spacers
Density functional theory analysis

ABSTRACT

To increase open-circuit voltage (V_{oc}), we introduced thieno[3,4-c]pyrrole-4,6-dione (TPD) moieties which has unsubstituted and substituted thiophene spacers. Poly(2,7-carbazole-alt-TPD) derivatives, namely PCDTTPD and PCDHTTPD, were copolymerized with 2,7-carbazole through Suzuki coupling reaction. An increase in the molecular weight and a decrease in the highest occupied molecular orbital (HOMO) energy level are confirmed. Steric hindrance caused by rotational dynamics was measured by density functional theory calculation. When the resulting polymers, PCDHTTPD, were used to fabricate a bulk heterojunction device with $PC_{71}BM$, V_{oc} increased to 0.84 V, whereas the short-circuit current density (J_{sc}) decreased to 0.93 mA/cm^2 because of poor charge dissociation.

1. Introduction

Semiconducting polymers have been used to develop useful materials such as organic photovoltaic cells. In the past few years, photovoltaic devices based on conjugated polymers have been extensively studied, and various polymer materials have been vigorously investigated in order to enhance the photovoltaic efficiency and oxidative stability of the most widely used polymer solar cells (PSCs), namely bulk heterojunction (BHJ)-type devices [1–6]. Even though numerous studies have been conducted on PSCs, their low power-conversion efficiency (PCE) remains the most important obstacle.

Thus, fine-tuning the opto-electronic properties of conjugated polymers, which act as the photo-active material in PSCs, is needed to increase the PCE. Therefore, the following ideal conditions are required: (1) a low band gap resulting from an enhanced absorption region, (2) low highest-occupied molecular orbital (HOMO) energy levels to achieve a high open-circuit voltage (V_{oc}), and (3) an increase in the molecular weight. In general, PCE values of BHJ PSCs are determined by the short-circuit current density (J_{sc}), V_{oc}, and fill factor (FF). In order to increase the PCE, it is necessary to improve the photon-harvesting properties of the PSCs by decreasing the band gap of the constituent conjugated polymers. With decrease in band gap, HOMO energy levels usually increase, whereas those of the lowest-unoccupied molecular orbital (LUMO) decrease. Thus, an increase in HOMO energy levels decreases V_{oc}, consequently reducing the PCE [7,8].

Carbazole and fluorene moieties act as donors of conjugated polymers that increase V_{oc} [9,10]. As reported by Leclerc et al., a well-known polymer, poly(*N*-9;-heptadecanyl-2,7-carbazole-alt-5,5-(4′,7′-dithienyl-2′,1′,3′-benzothiadiazole) (PCDTBT), was polymerized and it showed a PCE of 3.6% [11]. Jassen et al. reported using a mixed solvent consisting of chlorobenzene and *o*-dichlorobenzene to control the thickness, and the PCE of PCDTBT increased to 5.8% [12]. Tao et al. enhanced the PCE of PCDTBT to 7.1% using a mixed solvent consisting of *o*-dichlorobenzene and dimethyl sulfoxide (DMSO) to control the morphology of PSCs [13]. Moreover, Heeger et al. achieved a PCE of 7.2% by using a metal oxide (TiO_x and MoO_x) as an interfacial layer [14].

Another moiety that increases V_{oc} is thieno[3,4-c]pyrrole-4,6-dione (TPD). TPD was first introduced as a conjugated polymer by Zhang [15]. It has a fused structure with both thiophene and pyrrole which plays the role of having quinoid structure and enhancing polarity, respectively. TPD has electron-withdrawing properties because of its molecular hybridization resulting from two carbonyl functional groups. And a solubility of TPD would be modified by using an amine-introduced alkyl group [16]. By using a mentioned-TPD, Leclerc et al. synthesized a polymer and reported a PCE of 5.5% for PSCs [17]. Fréchet et al. polymerized TPD by using different alkyl chains which introduced to nitrogen atoms. In

* Corresponding author. Tel.: +82 2 450 3498; fax: +82 2 444 0765.
E-mail address: dkmoon@konkuk.ac.kr (D.K. Moon).

1226-086X/$ – see front matter © 2013 The Korean Society of Industrial and Engineering Chemistry. Published by Elsevier B.V. All rights reserved.
http://dx.doi.org/10.1016/j.jiec.2013.03.035

particular, polymers containing TPD derivatives with an octyl chain were used to fabricate PSC devices. These devices showed a PCE of 6.8% [18]. Tao et al. synthesized a polymer containing dithienosilole. By adding diiodooctane (DIO), a PCE of 7.3% was achieved [19]. Also, Reynolds et al. synthesized a polymer using dithienogermole, and the PSC with additive, DIO, showed a PCE of 7.3% [20].

Leclerc et al. synthesized TPD moieties with unsubstituted and alkyl-substituted thiophene spacers, and both TPD moieties were polymerized with BDT. They also reported on the type, length, and position of the side chains. According to their results, the polymers containing TPD with unsubstituted thiophene spacer were not soluble in organic solvent. By introducing an octyl chain to the 3-position of thiophene and TPD, the resulting polymer achieved a molecular weight of 131 kDa and a PCE of 3.9%. The molecular weight of the polymer, in which a shorter ethyl chain was introduced at the same position as thiophene, decreased by a factor of 10 (11.6 kDa) and a PCE of 3.5% was achieved [21].

Also, Leclerc et al. reported copolymers which contains 2,7-carbazole and TPD with unsubstituted and substituted thiophene spacers, respectively [22]. These polymers were then used to fabricate BHJ PSCs with a (6,6)-phenyl C_{61}-butyric acid methyl ester ($PC_{61}BM$) acceptor, and a V_{oc} of more than 1.0 V was reported. In addition, Leclerc et al. fabricated **PCDTTPD** with an unsubstituted thiophene spacer and it showed the highest PCE of 1.82%. However, they neglected the effect of the side chain and did not performed the optimization of device fabrication using (6,6)-phenyl C_{71}-butyric acid methyl ester ($PC_{71}BM$).

In this study, we synthesized TPD with unsubstituted and substituted thiophene spacers copolymerized with 2,7-carbazole, namely **PCDTTPD** and **PCDHTTPD** (see Scheme 1). We measured the opto-electronic properties and performed quantum mechanical analysis according to density functional theory (DFT). Also, we fabricated BHJ PSCs with $PC_{71}BM$ and determined the photovoltaic properties and morphological differences. As a result, a V_{oc} of more than 0.8 V and a low PCE (0.53%) were confirmed.

Table 1
Molecular weight of polymers and degree of polymerizations.

Polymer	Yield (%)	Mn[a] (kDa)	Mw[a] (kDa)	PDI[a]	Degree of polymerization[b]
PCDTTPD	6	5.4	6.8	1.26	6
PCDHTTPD	25	9.1	13.0	1.48	9

[a] Determined by GPC in tetrahydrofuran (THF) using polystyrene standards.
[b] Calculated values which Mn is divided by molecular weight of repeating units.

2. Results and discussion

Scheme 1 shows a schematic of the general synthetic routes of both the monomers and polymers used in this study. We synthesized these polymers through a palladium-catalyzed Suzuki coupling reaction using **PCDTTPD** and **PCDHTTPD**. Polymerization was performed under a 2 M aqueous potassium carbonate solution, using toluene as a solvent with $Pd(PPh_3)_4(0)$ as a catalyst and Aliquat 336 as a surfactant at 100 °C for 48 h. Once the polymerization was completed, the samples were end-capped with bromobenzene and phenyl boronic acid. The polymer yields were 6% and 25% with **PCDTTPD** and **PCDHTTPD**, respectively. The obtained powders were again purified in a Soxhlet apparatus with methanol, acetone, and chloroform. Finally, the chloroform-soluble portion was reprecipitated in methanol. **PCDTTPD** revealed a red powder, whereas **PCDHTTPD** showed orange powders **PCDHTTPD** was readily soluble in THF, toluene, $CHCl_3$, chlorobenzene, and *o*-dichlorobenzene. On the other hand, **PCDTTPD** was slightly soluble in only heated THF and showed poor solubility in the other organic solvent even at elevated temperature. The structures of the obtained polymers were confirmed with ^{1}H-NMR spectra (Fig. S1 in ESI). As shown in Table 1, **PCDTTPD** and **PCDHTTPD** revealed the number-average molecular weights of 5.4 and 9.1 kDa and polydispersity index (PDI) distribution of 1.26 and 1.48, respectively. Because of the thiophene-introduced hexyl chain at the 3-position, **PCDHTTPD** showed an increased degree of polymerization and molecular weight. Also, the thermal stability of

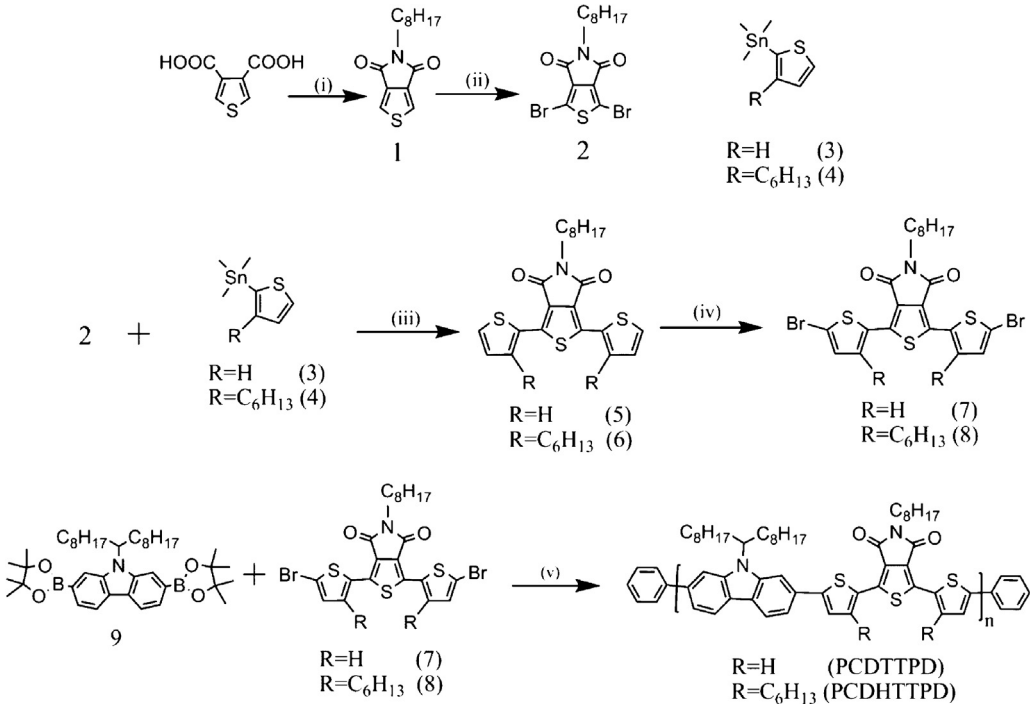

Scheme 1. Synthesis of monomers and polymers. Condition and reagents: (i) AcO_2 140 °C, toluene, $C_8H_{17}NH_2/SOCL_2$ 4 h; (ii) CF_3COOH H_2SO_4, NBS, RT; (iii) THF, Pd(II), 24 h; (iv) AcOH-$CHCL_3$(v/v, 1:1), NBS, 0 °C then 55 °C; (v) toluene, Pd(0), 90 °C.

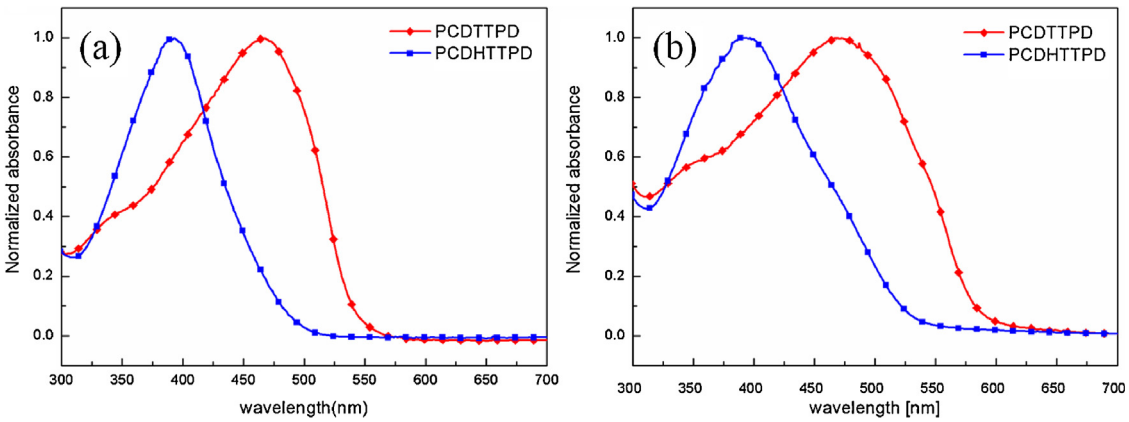

Fig. 1. UV–vis absorption spectra of PCDTTPD and PCDDHTTPD (a) in $CHCl_3$ and (b) in film.

PCDHTTPD was measured by thermogravimetric analysis (TGA), in which 5% thermal weight loss was confirmed at 355 °C [23]. Leclerc et al. reported thermal stabilities of the polymer which have similar structures, at 450 and 425 °C, respectively. Thus, the enhanced molecular weight and good thermal stability obtained in this study are well matched with those reported by Leclerc et al. [21,22].

Fig. 1 shows the UV–vis spectra of polymers in the solution and film state, and the data are summarized in Table 2. The maximum absorption peak (λ_{max}) of **PCDTTPD** was 466 nm in solution. As compared to the solution state, the results were red-shifted by 3 nm (λ_{max} = 469 nm) in the film. Because of this red-shift, **PCDTTPD** film showed π-stacking caused by the aggregation of particles in the solid state. Owing to a shoulder peak at ~550 nm, intramolecular π–π stacking occurs in the **PCDTTPD** film [24]. The absorption edge of **PCDTTPD** film was 590 nm while the calculated optical band gap was 2.10 eV, indicating a moderate band gap. On the other hand, λ_{max} of **PCDHTTPD** was 393 nm in solution. In the solid state, the λ_{max} of **PCDHTTPD** was blue-shifted by 2 nm (391 nm) as compared to its solution state. Thus, as compared to **PCDTTPD**, the UV–vis spectra of **PCDHTTPD** were blue-shifted as 73 nm in solution and as 78 nm in the film. These blue shifts occurred because of a disordered phase in the solution and film states [25] and the increased rotational dynamics of thiophene, which twisted the π-orbital in an out-of-plane direction [26]. The absorption edge of **PCDHTTPD** film was 532 nm and the calculated optical band gap was 2.33 eV, which is larger than that of **PCDTTPD** by 0.23 eV.

Fig. S2 shows the cyclic voltammograms (CVs) of the **PCDTTPD** and **PCDHTTPD** films, and the data are summarized in Table 2. The CVs were measured by using 0.1 M tetrabutylammonium hexafluorophosphate in acetonitrile solution. The **PCDTTPD** and **PCDHTTPD** films showed oxidation onset potentials of +1.10 V and +1.15 V, respectively. The HOMO levels of **PCDTTPD** and **PCDHTTPD** were calculated to be −5.43 eV and −5.48 eV, respectively. Thus, the HOMO level of **PCDHTTPD** is decreased as 0.05 eV by the electron-donating hexyl chain. These results are well matched with the results of our previous studies, in which a decrease in the HOMO energy level occurred owing to an increase in electron-donating groups [27]. The LUMO levels between the HOMO energy levels and the optical band gaps were also calculated, and the LUMO energy levels of **PCDTTPD** and **PCDHTTPD** were found to be −3.33 and −3.15 eV, respectively. The low LUMO energy level of **PCDTTPD** (−3.33 eV) had a smaller gap than that of $PC_{71}BM$ (−4.00 eV) [28]. In addition, the low LUMO energy level enables easy charge dissociation, and an enhanced J_{sc} might be expected when PSCs are fabricated using **PCDTTPD**. Consequentially, the electron-donating hexyl chain lowers the HOMO energy level and electron-withdrawing properties, thereby enhancing the band gap and the LUMO energy level. This change in the LUMO energy level is well matched with the results of a previous study of Leclerc (−3.74 eV → −3.39 eV) [25].

To better understand the electronic properties of the synthesized polymers, the molecular geometries and electron density of states were simulated using DFT. DFT was calculated using Gaussian 09 for a hybrid B3LYP correlation functional and a split-valence 6-31G(d) basis set. The calculated HOMO and LUMO orbitals of compound 5 and 6 in Scheme 1, namely DTTPD and DHTTPD, are shown in Fig. S3. The HOMO energy level of DHTTPD (−5.73 eV) is lower than that of DTTPD (−5.53 eV) because of the hexyl chain, which has electron-donating characteristics. In addition, introducing a side chain to the synthesized polymers decreases their electron-withdrawing properties. Thus, the LUMO level of DHTTPD is evaluated to be −1.83 eV. Only one repeating unit of each polymer was selected as a calculation model. The calculated HOMO energy levels are summarized in Table 2 and shown in Fig. 2. The calculation results of the polymers were similar to those obtained for the TPD derivatives. The HOMO energy level (−5.25 eV) of **PCDHTTPD** with a hexyl chain was higher as 0.07 eV than that of **PCDTTPD** (−5.18 eV).

According to the calculations, the LUMO energy level of **PCDHTTPD** with a hexyl chain increased as 0.29 eV and was

Table 2
Optical and electrochemical data of all polymers.

	UV–vis absorption				Cyclic voltammetry			DFT
	Solution		Film					
	λ_{max} (nm)	λ_{max} (nm)	λ_{onset} (nm)	E_g^{op} (eV)[a]	$E_{ox,onset}$ (V)/HOMO (eV)	$E_{red,onset}$ (V)/LUMO (eV)	LUMO[b] (eV)	Calcd HOMO (eV)
PCDTTPD	466	469	590	2.10	1.10/−5.43	−0.73/−3.60	−3.33	−5.18
PCDHTTPD	393	391	532	2.33	1.15/−5.48	−1.05/−3.28	−3.15	−5.25

[a] Calculated from the intersection of the tangent on the low energetic edge of the absorption spectrum with the baseline.
[b] LUMO = HOMO + E_g^{op}.

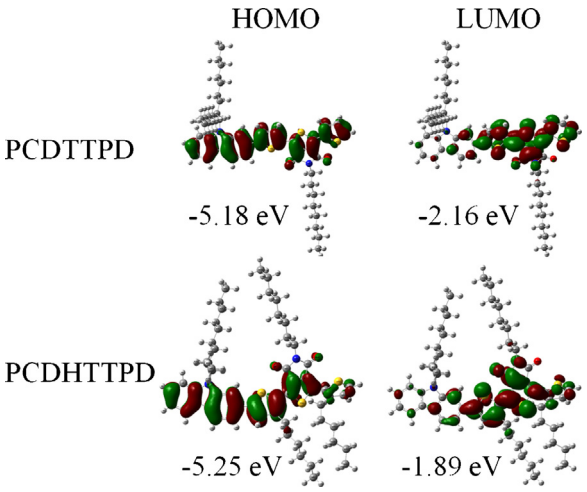

Fig. 2. Gaussian calculation of PCDTTPD and PCDHTTPD.

confirmed as −1.89 eV. In addition, the results of the Gaussian calculation showed the same tendency as observed with the CVs. Therefore, by introducing a hexyl chain, the HOMO energy level is decreased and the LUMO energy level is increased.

In the optimized structure of one repeating unit, the dihedral angle between the central TPD and the two thiophene derivatives was measured. The dihedral angle of **PCDTTPD** was 180°. However, the tilt angles of **PCDHTTPD** were 138° and 144°. These phenomena were explained by the blue-shift observation in the UV–vis spectra. The potential energy surfaces of the dihedrals in DTTPD and DHTTPD scanned as shown in Fig. 3 [29]. DTTPD showed the lowest relative energy at 0° and 180°. However, DHTTPD showed a high relative energy at approximately 180°. As a result, DTTPD exhibits a planar structure; however, DHTTPD shows a stable structure only when the tilt angle is 140°. These results match with those of UV–vis spectra.

To determine the photovoltaic properties as a function of the side chains, BHJ PSCs were fabricated. Fig. 4 reveals the characteristics of BHJ PSCs, and the results of the fabricated PSCs are listed in Table 3. The photovoltaic properties of all the polymers were evaluated after fabricating the PSC devices with an ITO/PEDOT:PSS/polymer:$PC_{71}BM$/BaF_2/Ba/Al structure. Leclerc et al. used only $PC_{61}BM$ as an acceptor [22], and thus different ratios of polymer/$PC_{71}BM$ need to be optimized. All fabricated devices were encapsulated in a glove box. The *J–V* characteristics were measured in ambient atmosphere with an active area of 4 mm^2. Fig. 4(a) reveals the *J–V* characteristic of PSCs fabricated with PCDDTTPD. A V_{oc} of 0.8 V, a J_{sc} of 2.7 mA/cm^2, and an FF of 28.4% were observed, yielding a PCE of 0.53%. In the case of **PCDHTTPD**, a low PCE of 0.18% was confirmed. However, the V_{oc} of **PCDHTTPD** (0.84 V) was increased by 0.04 V because of the decreased HOMO energy level owing to the hexyl chain. The increased V_{oc} might be because of a decreased dark saturation current (J_0). A decrease of J_0 is occurred by the reduction of nonradiative pathways and the increase of the carrier lifetime [22]. Thus, as shown in Table 3, the calculated J_0 of **PCDHTTPD** is smaller than that of **PCDTTPD** by an order of one and the V_{oc} of **PCDHTTPD** is enhanced. Also, because of the increased

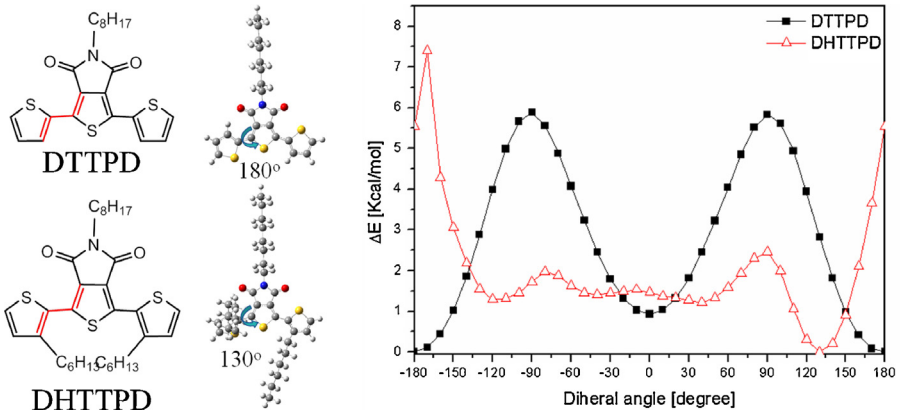

Fig. 3. Backbone conformation of DTTPD and DHTTPD.

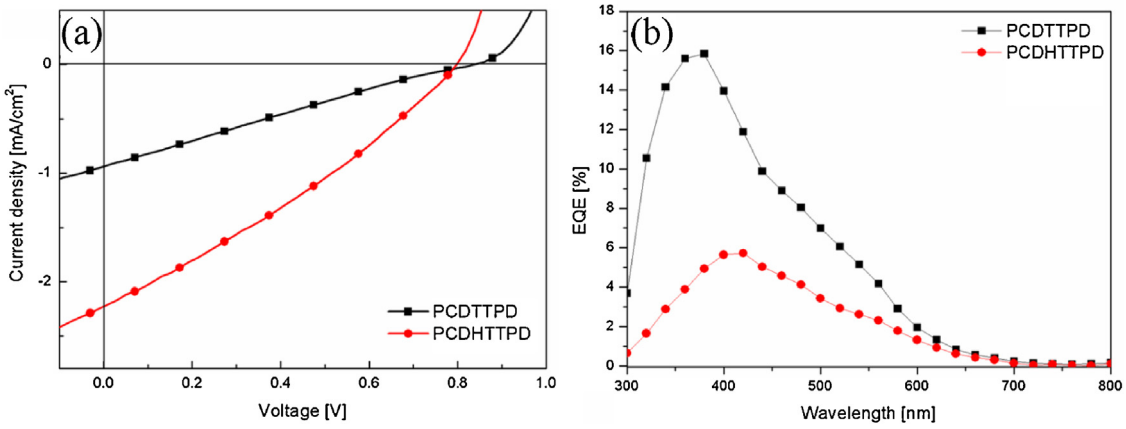

Fig. 4. (a) The *J–V* characteristics and (b) the IPCE spectra of BHJ solar cells with the device.

Table 3
Photovoltaic performances of polymers.

polymer	$PC_{71}BM$ ratios	V_{oc} (V)	J_{sc} (mA/cm^2)	FF (%)	PCE (%)	J_0 (A/cm^2)[a]
PCDTTPD	1:1	0.80	2.20	30.2	0.53	6.60×10^{-17}
PCDHTTPD	1:1	0.84	0.93	23.7	0.18	0.58×10^{-17}

[a] Calculated from Ref. [22].

band gap, LUMO level, and steric hindrance, efficient charge transfer and dissociation do not occur. Therefore, in spite of having a high molecular weight, **PCDHTTPD** shows a low J_{sc} (0.93 mA/cm^2). Fig. 4(b) reveals the incident photon-to-charge carrier efficiency (IPCE) in the polymers. The IPCE in all the polymers exhibited a light absorbance at 300–700 nm. In particular, the IPCE value of **PCDTTPD** exhibited an IPCE of 16% at 380 nm, whereas **PCDTTPD** exhibited an IPCE of 5.7% at 420 nm

The morphology of the polymer/$PC_{71}BM$-blend film was measured with atomic force microscopy (AFM), and the results are shown in Fig. 5. The dark-colored and light-colored areas correspond to PCBM domains and polymers, respectively [7]. PCDTTPD and $PC_{71}BM$ showed well-defined phase separation; on the other hand, PCDHTTPD exhibited macrophase separation. It means that **PCDHTTPD** did not well-mixed with $PC_{71}BM$ due to steric hindrance. Therefore, **PCDHTTPD** and $PC_{71}BM$ formed each domain. A polymer has lower density compared to PCBM, generally. As a result, polymer-only domain showed above the surface and increased root mean square (RMS) roughness [30]. Thus, **PCDHTTPD** showed a large RMS roughness of 1.87 nm as compared to that of **PCDTTPD** (0.53 nm) because of high steric hindrance resulting from the hexyl chain.

3. Experimental

3.1. Materials

All starting materials were purchased from Sigma Aldrich and Alfar Aesar, and used without further purification. Toluene and tetrahydrofuran (THF) were distilled from benzophenone and sodium. Other reagents and chemicals were used as received. 1,3-dibromo-5-(octyl)thieno[3,4-c]pyrrole-4,6-dione(2) [17], 2,7-bis(4′,4′,5′,5′-tetramethyl-1′,3′,2′-dioxab-oxaborolan-2′-yl)-N-9″-heptadecanylcarbazole(9) [31], 2-trimethylstannyl-3-hexyl thiophene(4) [32] were prepared as described in the literatures.

3.1.1. 1,3-dibromo-5-octyl-5H-thieno[3,4-c]pyrrole-4,6-dione (2)

5-octylthieno[3,4-c]pyrrole-4,6-dione (2.0 g, 7.537 mmol) was dissolved in a mixture of sulfuric acid (11.5 mL) and trifluoroacetic acid (112 mL). While stirring, NBS (4.047 g, 22.61 mmol) was added in five portions to the solution and the reaction mixture was stirred at room temperature overnight. The brown-red solution was diluted with water (100 mL). The mixture was extracted with dichloromethane. The organic phase was dried over anhydrous sodium sulfate and the solvent was evaporated under reduced pressure. The crude product was purified by column chromatography using dichloromethane/hexanes (1:1 ratio) to afford 2.5 g of the title product as white

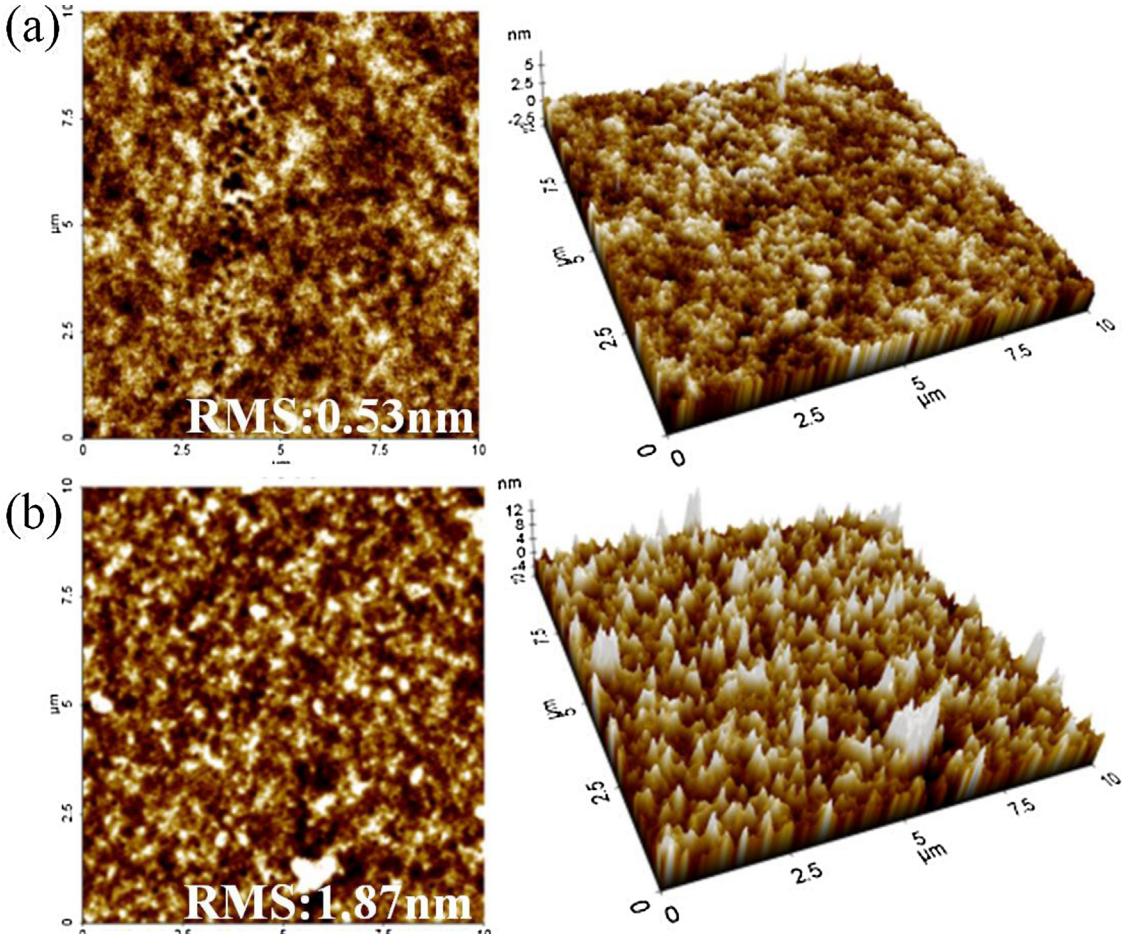

Fig. 5. Topographic AFM images of (a) PCDTTPD:$PC_{71}BM$ 1:1 (10 μm × 10 μm) and (b) PCDHTTPD:$PC_{71}BM$ 1:1 (10 μm × 10 μm).

needles (yield = 78%). mp:104°C, ^{1}H NMR(400 MHz, $CDCl_3$, δ): 3.59 (t, 2H, J = 7.4 Hz); 1.63 (m, 2H); 1.26 (m, 10H); 0.87 (t, 3H, J = 7.0 Hz).

3.1.2. 2-trimethylstannane-3-hexylthiophene (4)

2-Bromo-3-hexylthiophene (12 g, 50 mmol) was dissolved in THF (41 mL), and the solution was cooled to −78 °C. Then a 2.0-M solution of lithium diisopropylamine in THF (28 mL, 56 mmol) was added dropwise for 1 h. After stirring for 1 h at −78°C, a 1.0 M solution of Me_3SnCl in THF (56 mL, 56 mmol) was added dropwise, and the mixture was stirred at −50°C for 2 h. Then the solution was allowed to warm up to room temperature and was stirred 24 h. After the reaction was completed, the reaction mixture was poured into water and extracted with ether. The organic phase was washed with brine several times and dried over Na_2SO_4. The solvents were removed through rotary evaporation to afford a brown liquid. The residue was reduced-distilled to produce a 15.6 g of the product as a colorless oil. (yield = 76%) ^{1}H-NMR (400 MHz, $CDCl_3$, δ): 6.85 (s, 1H); 2.55 (t, J = 7.6 Hz, 2H); 1.56 (t, J = 7.2 Hz, 2H); 1.31 (m, 6H); 0.88 (t, J = 6.8 Hz, 3H); 0.36 (t, J = 27.6 Hz, 9H)

3.1.3. 5-octyl-1,3-di(thiophen-2-yl)-4H-thieno[3,4-c]pyrrole-4,6(5H)-dione (5)

Compound 2 (1.0 g, 2.363 mmol) was dissolved into anhydrous THF(95 mL). 2-(tributylstannyl)thiophene (2.64 g,7.090 mmol), and bis(triphenylphosphine) palladium(II) dichloride (10 mg, 6%) were added to the reaction mixture. The solution was refluxed for 24 h then cooled and poured into water. The mixture was extracted twice with dichloromethane. The organic phases were combined, washed with brine, and dried over anhydrous sodium sulfate. The solvent was removed under reduce pressure and the crude product was purified by column chromatography using dichloromethane:hexanes as the eluent (ratio 1:1) to afford 1 g of the product as a green powder (yield = 98%). ^{1}H NMR (400 MHz, $CDCl_3$, δ): 8.33 (d, 2H); 7.78 (d, 2H); 7.34 (t,2H, J = 4.2 Hz); 3.83 (t, 2H, J = 7.1 Hz); 1.89 (m, 2H); 1.53–1.47 (m,10H); 1.05 (t, 3H, J = 7.2 Hz).

3.1.4. 1,3-bis(3-hexylthiophen-2-yl)-5-octyl-4H-thieno[3,4-c]pyrrole-4,6(5H)-dione (6)

Compound 6 was synthesized with the same procedure of compound 5 by using 1.0 g of the compound 2 and 1.75 g of the compound 4. The crude product was obtained 1.0 g of the orange sticky solid. (yield = 71%) ^{1}H NMR (400 MHz, $CDCl_3$, δ): 7.42 (d, 2H, J = 5.2 Hz); 7.02 (d, 2H, J = 5.2 Hz); 3.63 (t, 2H, J = 7.2 Hz); 2.80 (t, 4H, J = 7.9 Hz); 1.66–1.63 (m, 6H); 1.30–1.25(m, 26H); 0.88 (t, 9H, J = 6.4 Hz).

3.1.5. 1,3-di(2′-bromothien-5′-yl)-5-octylthieno[3,4-c]pyrrole-4,6-dione (7)

Compound 5 (1 g, 2.328 mmol) was dissolved in a mixture of acetic acid and chloroform (78 mL) (ratio 1:1). The solution was cooled to 0 °C and kept in the dark. *N*-Bromosuccinimide (1.245 g, 6.983 mmol) was added to the solution in several portions. The cooling bath was removed and the reaction was stirred at ambient temperature for 24 h. The reaction solution was poured into water and extracted several times with chloroform. The organic phases were combined, washed with brine, and dried over anhydrous sodium sulfate. The solvent was removed under reduced pressure and the crude product was purified by column chromatography using dichloromethane:hexanes as the eluent (ratio 1:1) to afford 0.3 g of the product as a bright yellow solid (yield = 21%) ^{1}H NMR (400 MHz, $CDCl_3$, δ): 7.65 (d, 2H, J = 4 Hz); 7.09 (d, 2H, J = 4 Hz); 3.64 (t, 2H, J = 6.9 Hz); 1.67 (m, 2H); 1.32–1.26 (m, 10H); 0.87(t, 3H, J = 5.4 Hz).

3.1.6. 1,3-di(5′-bromo-3-hexylthien-2′-yl)-5-octylthieno[3,4-c]pyrrole-4,6-dione (8)

Compound 8 was synthesized with the same procedure of compound 7. By using compound 6 (1.67 g, 2.793 mmol), a mixture of acetic acid and chloroform (93 mL) (ratio 1:1) at 0 °C, and *N*-bromosuccinimide (1.494 g, 8.379 mmol). After the addition of NBS, the cooling bath was removed and the reaction was stirred at ambient temperature for 24 h. The solution was then heated up to 55 °C for 24 h. The reaction was carefully monitored by thin layer chromatography (TLC). The reaction mixture was cooled and poured into water. The mixture was extracted three times using chloroform. The chloroform parts were combined, washed with brine, and dried over anhydrous sodium sulfate. The crude product was purified by column chromatography using dichloromethane:hexanes as the eluent (ratio 1:1) to afford 2 g of the product as a yellow solid (yield = 94%). ^{1}H NMR (400 MHz, $CDCl_3$, δ): 6.96 (s, 2H); 3.60 (t, 2H, J = 7.1 Hz); 2.75– 2.71 (t, 4H, J = 7.6 Hz); 1.64–1.60 (m, 6 H); 1.30–1.25 (m, 30 H); 0.88–0.84 (t, 9H, J = 5.7 Hz).

3.2. General polymerizations through the Suzuki coupling reaction

To a mixture of tetrakis(triphenyl-phosphine) Pd(0) (12 mg, 0.010 mmol, 2mol%), 2,7-Bis(4′,4′,5′,5′-tetramethyl-1′,3′,2′-dioxaborolan-2′-yl)-N-9″-heptadecanylcarbazole(9) (0.336 g, 0.511 mmol), and equivalent of halogen compound, e.g. compound 7 and 8, was added a degassed mixture of toluene (lmonomerl = 0.06 M) and 2 M K_2CO_3 aqueous solution (3:2 in volume). The mixture was vigorously stirred at 85–90 °C for 48 h under the nitrogen. After the mixture was cooled to room temperature, it was poured into the methanol. A powder was obtained by filtration was reprecipitated with methanol several times. The polymer was further purified by washing methanol and acetone, respectively, in a Soxhlet apparatus for 24 h and only chloroform portion is dried under reduced pressure at 50 °C [13].

3.2.1. Poly[2,7-bis-(N-heptadecan-9-yl)-carbazole-alt-1,3-di(2′-thien-5′-yl)-5-octylthieno[3,4-c]pyrrol- e-4,6-dione] (PCDTTPD)

Red solid 0.018 g (yield = 6%). ^{1}H NMR (400 MHz, $CDCl_3$, δ): 8.24–7.37 (m, 30H), 4.66 (m, 3H), 2.63(m, 5H), 2.34(m, 3H), 1.99–0.60(m, 158H)

3.2.2. Poly[2,7-bis-(N-heptadecan-9-yl)-carbazole-alt-1,3-di-5′-(3-hexylthien-2′-yl)-5-octylthieno[3,4-c]pyrrole-4,6-dione] (PCDHTTPD)

Orange solid 0.1 g (yield = 25%) ^{1}H NMR (400 MHz, $CDCl_3$, δ): 8.08–7.32 (m, 17H), 4.62(s, 2H), 2.46–0.48 (m, 226H)

3.3. Measurements

The ^{1}H-NMR (400 MHz) spectra were recorded using a Brüker AMX400 spectrometer in $CDCl_3$, and the chemical shifts were recorded in units of ppm with TMS as the internal standard. The absorption spectra were recorded using an Agilent 8453 UV–visible spectroscopy system. The solutions that were used for the UV–visible spectroscopy measurements were dissolved in chloroform at a concentration of 10 μg/mL. The films were drop-coated from the chloroform solution onto a quartz substrate. All of the GPC analyses were carried out using THF as the eluent and a polystyrene standard as the reference. The TGA measurements were performed using a TG 209 F3 thermogravimetric analyzer. The cyclic voltammetric waves were produced using a Zahner IM6eX electrochemical workstation with a 0.1 M acetonitrile (substituted with nitrogen for 20 min) solution containing tetrabutylammonium hexafluorophosphate (Bu_4NPF_6) as the electrolyte at a constant scan rate of 50 mV/s. ITO, a Pt wire, and silver/silver chloride [Ag in 0.1 M KCl] were used as the working, counter, and reference electrodes, respectively. The

electrochemical potential was calibrated against Fc/Fc+. The HOMO levels of the polymers were determined using the oxidation onset value. Onset potentials are values obtained from the intersection of the two tangents drawn at the rising current and the baseline changing current of the CV curves. The LUMO levels were calculated from the differences between the HOMO energy levels and the optical band-gaps, which were determined using the UV–vis absorption onset values in the films. The current density–voltage (*J*–*V*) curves of the photovoltaic devices were measured using a computer-controlled Keithley 2400 source measurement unit (SMU) that was equipped with a Class A Oriel solar simulator under an illumination of AM 1.5G (100 mW/cm^2). Topographic images of the active layers were obtained through atomic force microscopy (AFM) in tapping mode under ambient conditions using an XE-100 instrument.

3.4. Device fabrication and characterization

All of the bulkheterojunction PV cells were prepared using the following device fabrication procedure. The glass/indiumtinoxide (ITO) substrates [Corning, Korea (10 Ω] were sequentially lithographically patterned, cleaned with detergent, and Ultrasonicated in deionizedwater, acetone and isopropyl alcohol. Then the substrates were dried on a hot-plateat120 °C for 10 min and treated with oxygen plasm for 10 min in order to improve the contact angle just before the film coating process. Poly(3,4-ethylene-dioxythiophene): poly(styrene-sulfonate) (PEDOT:PSS,-BaytronP 4083 BayerAG) was passed through a 0.45 μm filter before being deposited on to ITO at a thickness of ca.32 nm by spin-coating at 4000 rpm and was dried at 120 °C for 20 min inside a glovebox. Composite solutions with polymers and PCBM were prepared using 1,2-dichlorobenzene(DCB). The concentration was controlled adequately in the 1.0wt% range, and the solutions were then filtered through a 0.45 mm PTFE filter and then spin-coated (500–2000 rpm, 30 s) on top of the PEDOT:PSS layer. The device fabrication was completed by depositing thin layers of BaF_2 (1 nm),Ba(2 nm), and Al (200 nm) at pressures of less than 10^{-6} torr. The active area of the device was 4 mm^2. Finally, the cell was encapsulated using UV-curing glue(Nagase, Japan).

In this study, all of the devices were fabricated with the following structure: ITO glass/PEDOT:PSS/polymer:PCBM/BaF_2/Ba/Al. The illumination intensity was calibrated using a standard Si photodiode detector that was equipped with a KG-5filter. The output photocurrent was adjusted match the photocurrent of the Si reference cell in order to obtain a powerdensity of 100 mW/cm^2. After the encapsulation, all of the devices were operated under an ambient atmosphere at 25 °C

4. Conclusions

In this study, two polymers, poly(2,7-carbazole-alt-TPD) derivatives of **PCDTTPD** and **PCDHTTPD**, were synthesized through a Suzuki coupling reaction and their physical and opto-electrical properties were analyzed. As compared to **PCDTTPD**, **PCDHTTPD** revealed enhanced solubility and molecular weight because of the presence of a hexyl chain. However, the electron-withdrawing nature of the polymer decreased while its rotational dynamics increased, leading to a high band gap of 2.33 eV. Both the solution and film states of **PCDHTTPD** were blue-shifted in the UV–vis spectra. Based on the change in the dihedral angle, **PCDHTTPD** having a planar structure was shown to be unstable. In addition, its HOMO level decreased, whereas the LUMO level is increased, results that matched well with the DFT calculations. When BHJ PSCs were fabricated and measured, the V_{oc} of **PCDHTTPD** increased to 0.84 V, whereas its J_{sc} decreased to 0.93 mA/cm^2 because of the difficult in achieving charge dissociation. In the PCDHTPD/PC_{71}BM-blend film, polymer aggregation occurred and the RMS of roughness increased to 1.87 nm.

Conflict of interest

The authors declare no competing financial interest.

Acknowledgments

This research was supported by a grant from the Fundamental R&D Program for Core Technology of Materials funded by the Ministry of Knowledge Economy, Republic of Korea. This work was supported by the National Research Foundation of Korea Grant funded by the Korean Government(MEST) (NRF-2009 – C1AAA001-2009-0093526).

Appendix A. Supplementary data

Supplementary data associated with this article can be found, in the online version, at doi:10.1016/j.jiec.2013.03.035.

References

[1] Y. Li, Accounts of Chemical Research 45 (5) (2012) 723.
[2] A. Mishra, C.-Q. Ma, P. Bäuerle, Chemical Reviews 109 (3) (2009) 1141.
[3] P.-L.T. Boudreault, A. Najari, M. Leclerc, Chemistry of Materials 23 (3) (2011) 456.
[4] P.M. Beaujuge, J.M.J. Fréchet, Journal of the American Chemical Society 133 (50) (2011) 20009.
[5] C.L. Chochos, S.A. Choulis, Progress in Polymer Science 36 (10) (2011) 1326.
[6] D.-H. Yun, et al. Journal of Industrial and Engineering Chemistry 19 (2) (2013) 421.
[7] J.-Y. Lee, et al. Journal of Materials Chemistry 21 (41) (2011) 16480.
[8] C. Du, et al. Macromolecules 44 (19) (2011) 7617.
[9] W. Pisula, et al., Organic Photovoltaics, Federal Republic of Germany, Germany, 2009, pp. 93–128.
[10] D. Jones, Organic Photovoltaics, Federal Republic of Germany, Germany, 2009 pp. 57–91.
[11] N. Blouin, et al. Journal of the American Chemical Society 130 (2) (2007) 732.
[12] V.S. Gevaerts, et al. Advanced Materials 24 (16) (2012) 2130.
[13] T.-Y. Chu, et al. Applied Physics Letters 98 (25) (2011) 253301.
[14] Y. Sun, et al. Advanced Materials 23 (19) (2011) 2226.
[15] Q.T. Zhang, J.M. Tour, Journal of the American Chemical Society 120 (22) (1997) 5355.
[16] R.S. Ashraf, et al. Chemical Communications 48 (33) (2012) 3939.
[17] Y. Zou, et al. Journal of the American Chemical Society 132 (15) (2010) 5330.
[18] C. Piliego, et al. Journal of the American Chemical Society 132 (22) (2010) 7595.
[19] T.-Y. Chu, et al. Journal of the American Chemical Society 133 (12) (2011) 4250.
[20] C.M. Amb, et al. Journal of the American Chemical Society 133 (26) (2011) 10062.
[21] A. Najari, et al. Advanced Functional Materials 21 (4) (2011) 718.
[22] A. Najari, et al. Macromolecules 45 (4) (2012) 1833.
[23] H.J. Song, et al. Journal of Industrial and Engineering Chemistry 17 (2) (2011) 352.
[24] X. Guo, et al. Journal of Materials Chemistry 22 (39) (2012) 21024.
[25] L.A. Cury, L.O. Ladeira, A. Righi, Synthetic Metals 139 (2) (2003) 283.
[26] R. Traiphol, N. Charoenthai, Synthetic Metals 158 (3/4) (2008) 135.
[27] J.-Y. Lee, et al. Journal of Polymer Science Part A: Polymer Chemistry 48 (21) (2010) 4875.
[28] H.-J. Song, et al. Macromolecules 45 (19) (2012) 7815.
[29] X. Lu, et al. Nature Communications 3 (2012) 795.
[30] S.W. Heo, et al. Solar Energy Materials and Solar Cells 114 (0) (2013) 82.
[31] N. Blouin, A. Michaud, M. Leclerc, Advanced Materials 19 (17) (2007) 2295.
[32] D.S. Chung, et al. Organic Electronics 11 (5) (2010) 899.